BioGecko Vol 12 Issue 03 2023

ISSN NO: 2230-5807

NEUTRAL NETWORK SOLID BASED WATER POLLUTION ASSEMBLY BY GOOGLE EARTH IMAGE

D.Shofia Priyadharshini[1],R.Breesha[2],R.Pranavesh[3],A.Sathish Kumar[3],C.Vinoth Kumar[3]
[1,2]Assistant Professor,Department of Electronics and Communication Engineering,Vel Tech High tech Dr.Rangarjan Dr.Sakunthala Engineering College,Chennai,India
[3]UG Scholar,Department of Electronics and Communication Engineering,Vel Tech High tech Dr.Rangarjan Dr.Sakunthala Engineering College,Chennai,India.

Abstract
Monitoring water quality is crucial for preserving freshwater supplies, but in-situ testing is costly. Remote sensing may be a more affordable option, yet it is challenging to estimate parameters that are not optically active. A Hierarchical-convolutional network of neurons (H-CNN) was created to depict the correlation between Landsat8 photos and water quality levels in order to solve this challenge. In order to deal with the paucity of in real-time measurement data, a transfer-learning technique was employed. The H-CNN model has been trained using in realtime water-quality data from public sources and geographically and temporal matching Landsat8 photos. This made it possible to group together the entire water body's surface quality. The following image was processed using MATLAB software, and the conjugation grading (CG), which was technique approach was used to distinguish between clean water and contaminated water.
Keywords: Water-Quality, Neural Network, In-situ, H-CNN, Conjugate Gradient Algorithm, Landsat8.

1 Introduction

Inland lakes hold a substantial amount of freshwater, which is essential for both human and environmental purposes. But because of escalating land use, population growth, and economic development, these lakes' water quality is in jeopardy. Due to pollution and a global freshwater deficit, this has become a problem. Monitoring the water condition and its characteristics in inland lakes is crucial for the preservation and management of freshwater resources. Levels of water quality are used as a standardised index for categorization and evaluation. The water quality measurements that were gathered for this study are in compliance with Chinese standards GB3838-2002, which was released by the country's Ministry of Urban and Agricultural Construction and Protection of the Environment in accordance with Chinese regulations governing environmental protection.

In contrast to regulations in the United States, Japan, and Europe, the classification standards for the water quality levels in GB3838-2002 are different. A parameter that surpasses its associated criteria with the highest correlation is chosen for the water-quality-level categorization in accordance with the single-factor technique. GB3838-2002 specified five different water-quality levels. One technique for checking the quality of the water is in-situ sampling and measurements. This type of water quality monitoring technique includes both manual measurement and automatically monitoring. Water-quality levels are computed using published water-quality parameters, which are mostly derived from in-situ sampling and measurement.

The conventional method for assessing or quantitatively predicting the water quality of rivers involves artificial sampling of chemicals related to that quality and the use of a point to replace an area adjacent to it in order to measure the concentration of a number of substances in small areas. This method is labour- and time-intensive, as well as inefficient. Local environmental protection departments use the centre point information to replace a 10 10 m2 region when detecting the statistics content level of water quality parameters since it is economically inefficient to conduct chemical analysis of various substances pertaining to water quality on portions of a river. Traditional chemical examination of 1% of the overall river area is time-consuming and requires several days.

Multispectral analysis, which makes use of tens of waves of various wavelengths, is a standard technique for assessing the levels of large-scale water contamination. Instead of using a quantitative prediction for the water quality-related parameters, Firrao -et-al. recommended a method based on ANN to predict the mycotoxin level that to water, which has a strong correlation with the number of algae and leads to excessive nutrients in the water. They used 10 different LED lights with emission at wavelengths ranging from 720-940 nm to classify the pollution level in several samples.

2 Related Works

We use water daily for many purposes in our homes and depend on potable water for our overall well-being and health. But only 3% of the water in the globe is fit for human consumption, and the majority of that water can be discovered in the glaciers and ice. Unexpectedly, just 1% of the water on Earth can be both accessible and drinkable. Therefore, it is essential to check the quality of the water earlier than using it for a variety of purposes.

In many regions of India, groundwater serves as the primary supply of drinking water. Due to the unreliability of municipal water supplies, groundwater is becoming increasingly important in metropolitan areas. A portable monitoring system was created employing networked pressure sensors to simplify and reduce the cost of groundwater research.The model of architecture of an Internet-enabled WSN system for managing water resources, which covers network deployment, setup, discovery, and maintenance, was the primary focus of the article. Three domains—the sensing, coordinating, and supervisory domainsare established inside the hardware infrastructure.

The sensing, coordinating, and supervisory domains make up the system. The study focuses on the network deployment, configuration, discovery, and maintenance of the Internet-enabled WSN, or wireless sensor network, system structure for water resource management. Water quality metrics including oxygen concentration and turbidity, which are crucial for policy choices regarding the upkeep and usage of significant water bodies, were predicted using supervised learning algorithms. The measurements are frequently erroneous for a variety of reasons, necessitating time and money from the USGS (United States Geological Survey) to look for abnormalities. The study made use of the support vector regression technique and gradient boosting with the XG Boost implementation.Over the course of three years, an overall 52,563 instances were gathered, allowing for more precise predictions and a deeper comprehension of the parameter to be used in relationships. Using a mix of approachable techniques and a close examination of the most recent data set, they want to demonstrate how machine learning is essential in this field of science. Consequently, it is demonstrated that supervised training can greatly streamline the USGS's process for validating data, saving the organization's valuable resources, and enhancing data fidelity.

Fisheries frequently gather information on water quality by taking water samples and analysing the resulting water colour. Because there are few opportunities to acquire images of water colour, this method is constrained and only allows for local water quality characteristics. Researchers have concentrated on information extraction with imperfect information and picture structure extraction to overcome this.In order to leverage local information and picture semantics to achieve excellent identification and restoration success rates, Chen and his colleagues have suggested techniques for finishing, reassembling, and restoring image information. A technique for accurately tracking essential target information in photographs has been developed by Xia and colleagues.

As an analysed object, water colour photographs are often obtained in a variety of ways. Up until now, water quality analysis has been carried out using a variety of processing images and AI algorithms. Water quality monitoring has made extensive use of remote sensing satellite picture capture. Utilising ANN, expert knowledge, a periodic a regression analysis model, and PCA-based response surface regression, it was possible to estimate and predict the presence of particular chemical components or organic matter in water using satellite image data.

In addition to these publications, several researchers have used hybrid algorithms or fundamental neural network (NN) related algorithms to address the issues associated with image-based water quality assessments. To analyse and forecast the water availability of picture data from surface water mapping, Isikdogan et al. used CNN in its entirety. To analyse contaminants in water with fish activity, Yuan et al. employed a hybrid algorithm combining long short-term memory (LSTM)

network and neural network (LSTM-NN). have used CNN with a structure of hierarchy to try and determine a correlation between inland lake remote sensing images and local water quality levels**.**

3 Proposed Methodology

In order to maximise the amount of information that can be gleaned from remote sensing photos, numerous image processing and analysis techniques have been created. The objectives of every project individually determine the specific approaches or algorithms that should be used. This section will look at several methods used frequently for evaluating and analysing remote sensing photographs.

Pre-Processing

In order to correct for any distortion brought on by the features of the imaging system and imaging settings, basic processing on the raw data is typically carried out before data analysis. Before the data is transmitted to the end-user, the ground system operators may perform various common corrective operations based on the user's requirements. These steps include a radiometric adjustment to fix unequal sensor response throughout the entire image and geometric correction to fix geometric distortion brought on by the rotation of the Earth and other imaging circumstances (such oblique viewing).A particular map projection system may require that the image be altered. Furthermore, ground control points (GCPs) are used to register the image to a precise map (geo-referencing) if the precise geographic location of an area on the image needs to be known.different imaging circumstances, including oblique viewing.

Image Enhancement

The visual appearance of the items in the image can be enhanced using image enhancement techniques like grey level stretching to increase contrast and spatial filtering to highlight edges in order to facilitate visual interpretation. Here is an illustration of an enhancement process is shown in Fig 1.

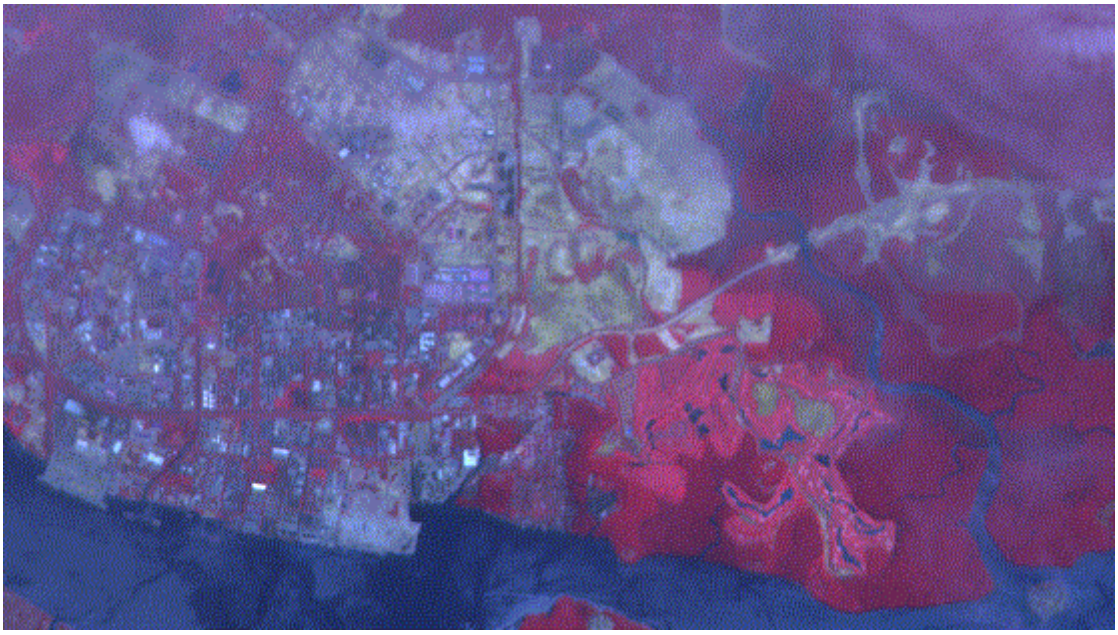

Fig 1: Enchament Process image

The unenhanced image seen above has a bluish hue that permeates the entire image and gives it a foggy appearance. This blurry appearance is caused by the atmosphere dispersing sunlight into the sensor's field of vision. Additionally, this effect lessens the contrast between various landcover types.

Before implementing any picture enhancement, it is helpful to look at the image histograms. The usable digital number range, or 0 to 255, is the histogram's x-axis. The number of pixels in the image with a certain digital number is represented on the y-axis. The following figures display the histograms for the three sections of this photograph.

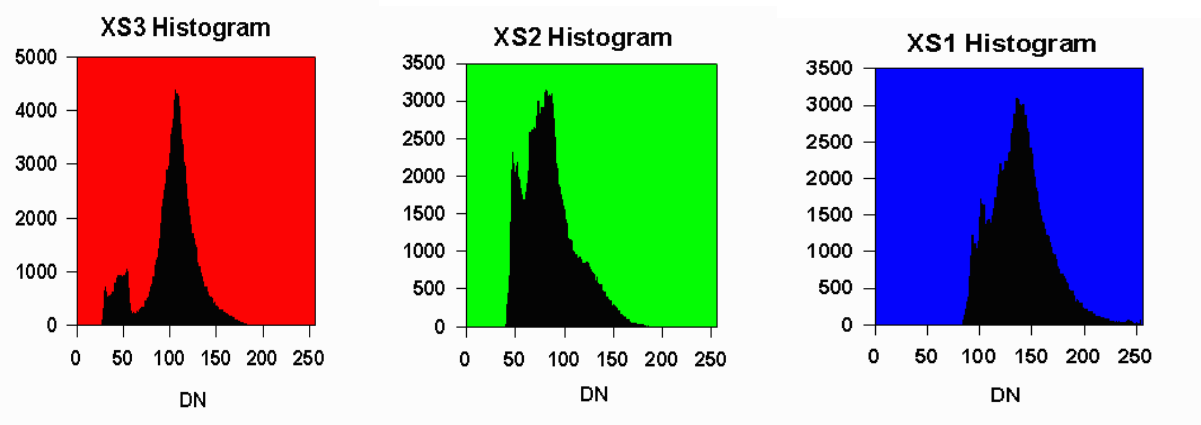

Fig 2: a) Histogram XS3(near infrared band)b) Histogram XS2(red band) c)Histogram XS1(green band)

Each histogram has a certain amount added to the right of it. The radiation that actually reflection from the ground changes as a result of the addition of the air scattering component. The shift is notably considerable because Rayleigh scattering provides more to the shorter wavelength of the XS1 band than to the longer wavelengths of the other two bands is shown in Fig 2.

The maximum digital number for each band is also not 255. The gain factor of the sensor was changed to take into account the possibility of encountering a very bright object. As a result, the vast majority of the image's pixels have digital values that are much lower than the maximum value of 255.Simple linear grey-level stretching can improve the image. The level threshold value used in this method is selected such that any pixel values below it are transferred to zero. Additionally, a higher threshold value is selected, causing all pixel values over it to be mapped to 255. The range of values for every other pixel is linearly interpolated to be between 0 and 255. Typically, values that are close to the lowest to highest pixel values of the image are selected for the lower and upper thresholds. TheFig 3 displays the Grey-Level Transformation table.

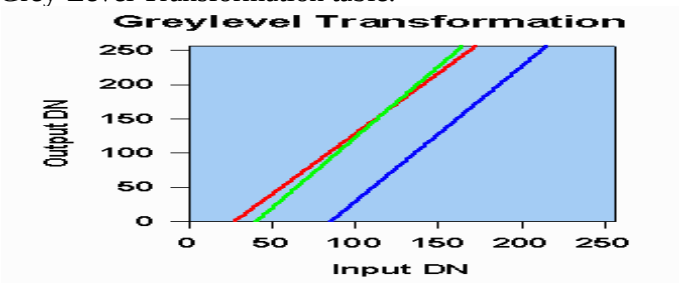

Fig3: Gray level Transformation

It displays the outcome of using the linear stretch. Except for a few spots near the top of the image, the obscure appearance has been mostly eliminated. Improvements have been made to the contrast between various features.

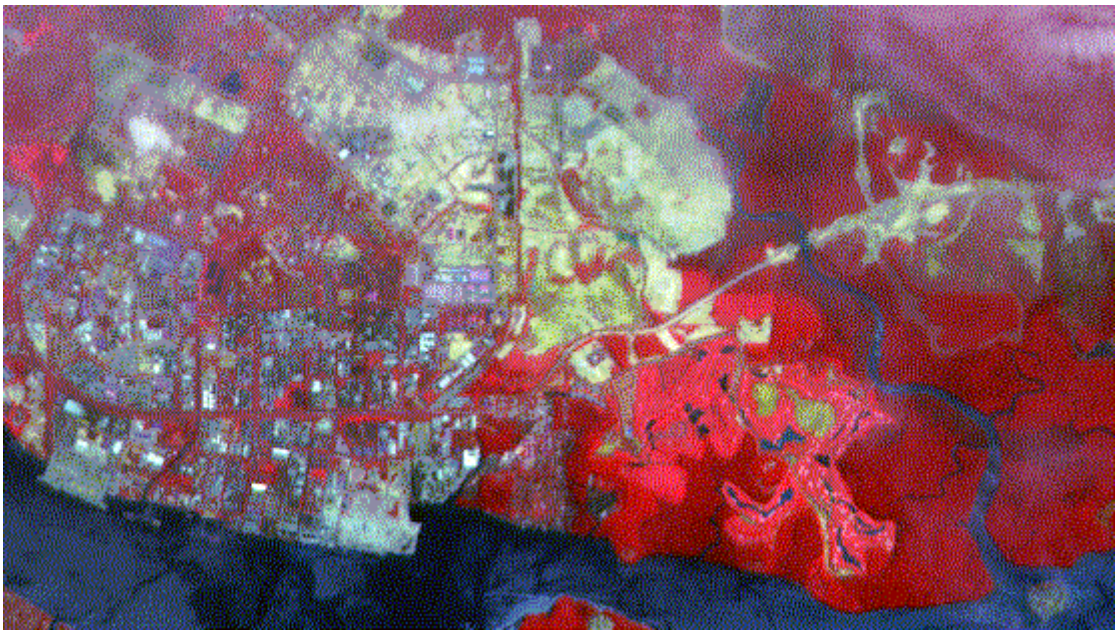

Fig 4: Rearrange the image

Water-Quality-Level Classification Based on Convolutional Neural Networks

Recent years have seen a boom in the study of convolutional neural networks, which have performed admirably in the processing of remote-sensing images. In contrast to SAEs and DBNs, CNN models do not mandate that input vectors be in a single dimension (1D). From multispectral data, CNNs can learn hierarchical and discriminative features. The development of deep learning is credited to AlexNet. AlexNet, the 2012 ILSVRC winner, is capable of learning both shallow and deep featuresIts classification performance benefits from optimisation techniques like overlapped samples and complicated ReLU activation functions. Compared to other CNN models like VGG and ResNet, the AlexNet model has a simpler structure. AlexNet works well with small input sizes. The following describes the framework of the convolutional neural network that was used for classifying the level of water quality: (1) The number of convolutional neural network layers cannot be high given the tiny input size of 21 _ 21 _ 7. The computationally complex nature of the CNN increases in direct proportion to the number of convolutional layersThrough testing and classification of water-quality, the optimal number of convolutional layers, ranging from 2 to 7, is found. (2) The stride and kernel sizes are both set to be modest. The performance of the AlexNet framework could be improved by changing the kernel sizes & stride. (3) In order to safeguard information, pooling layers are deleted its shown in fig 4.

Other settings included applying a Rectified Linear Unit (ReLU) as each layer's activation function. Similar to the AlexNet model, three fully linked layers were also placed behind convolutional layers. The output of the final completely connected layer was supplied into a 3-way soft max layer that corresponds to the three water-quality class labels of Class A, Class B, and Class C in order to balance the quantity of each water-quality levelClass A of the GB3838-2002 standard, which encompasses Classes I and II, denotes water of good quality. Class B, which corresponds to Class III of the GB3838-2002 standard, denotes water used for industry and fishery.

Class C water, which includes Class IV, Class V, and above, can be used for leisure and irrigation but is unfit for human consumption. There was a dropout method used among fully connected layers. In order to stop the CNN from becoming too well fitted, the dropout strategy randomly removes units as well as their connections.Figure 5 depicts an architecture with 4 convolutional layers and 3 fully connected layers its shown in fig 5.

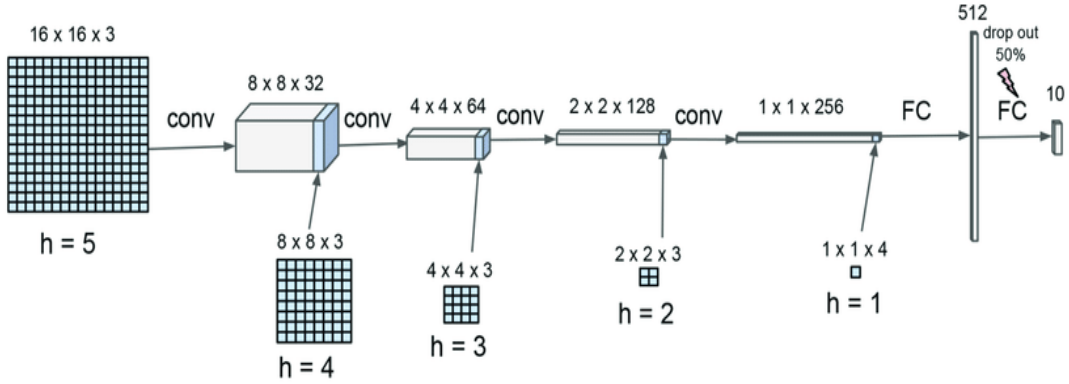

Fig 5: Neural Network

Transfer Learning

It is challenging to right away train a good CNN model when the objective job only has a tiny amount of tagged data. Transfer learning can be used to solve the issue. Transmit learning is a technique for enhancing target task performance without overfitting by using knowledge gained from source activities. Additionally, it saves time by avoiding the random setting up of model weights during training. It works particularly well for a deep architecture. Given that there are fewer in situ data for Chaohu Lake than for Erhai Lake, transferred learning using the CNN model developed for Erhai Lake was used to categorise the water quality level for Chaohu Lake. Weights were adjusted to better suit the data from Chaohu Lake on the model that had been trained in Erhai Lake. The outcomes of the experiment show how reliable and efficient our CNN model .

Im2Double Process In Image

Fig 6: Alternating Image

The input picture may be a multidimensional array, scalar, vector, or matrix of numbers. Based on whether it is a grayscale or true colour (RGB) image, an indexed image, or a binary image, it can be of several sorts. Images that are indexed can be of the kinds uint8, uint16, double, logical, single, or int16 while images that are grayscale or true colour can be of the types uint8, uint16, double, or logical. The kind of binary images must be rational. If the Parallel Computing Toolbox is installed, the function im2double can convert the input image to a GPU if it is a gpuArray its shown in fig 6.

Fig 7 : Im2double Image Process

Example

An image is convert the image into 0011 or some value to identifier the correct rate of colour in image it shown in fig 7.

RBG

The function rgb2gray (RGB) takes a true colour image RGB as input and converts it to a grayscale image I. The rgb2gray function achieves this by removing the hue and saturation information from the image while retaining only the luminance information. The rgb2gray function can accelerate performance by performing this conversion on a GPU if the Parallel Computing Toolbox is enabled.As an example, the function call rgb2gray(map) returns a grayscale colormap that is equivalent to the input colourmap map.

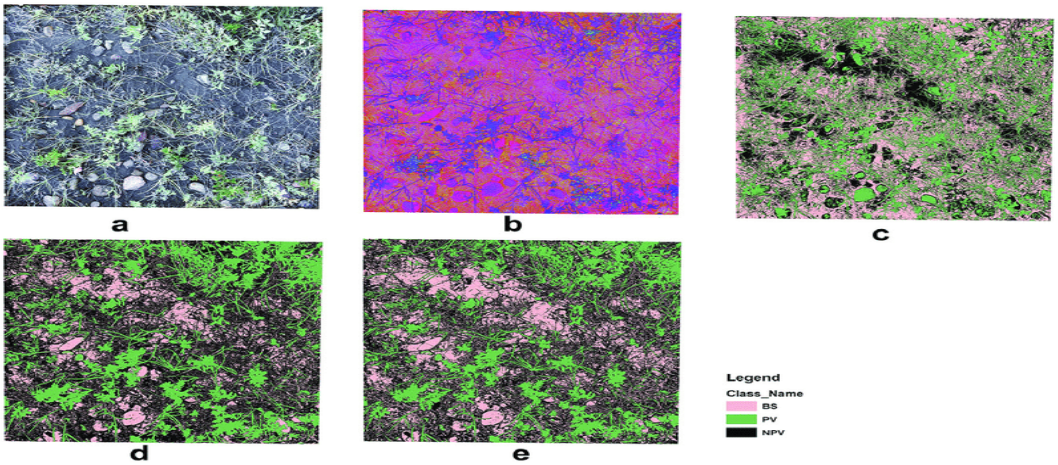

Fig 8: RGB Coverted Images

Algorithms

The function rgb2gray converts RGB values to grayscale values by taking a weighted sum of the R, G, and B components using the formula:0.2989 * R + 0.5870 * G + 0.1140 * B.These weights are the same ones that the Image Processing Toolbox's function rgb2ntsc uses to calculate the Y component. When rounded to three decimal places, the coefficients used in rgb2gray to create grayscale values are also the same as those used in Rec.ITU-R BT.601-7 to determine brightness (E'y) its shown in fig 8. The Rec.ITU-R BT.601-7 formula for calculating E'y is: 0.299 * R + 0.587 * G + 0.114 * B

4 Results And Discussions

Based on the created CNN, the multispectral remote sensing photos were divided into three water-quality levels. From 41 frames of Landsat8 images taken at Erhai Lake between January 2014 and October 2018, training samples for CNN were chosen. The training set to the test set ratio was 4:1. There were 128, 256, or 512 kernels for each convolutional layer. Stride was set to 1, and the kernel

size was 3 _ 3. The dropout method for the first two layers that are completely linked was set to 50%, and there were 512, 256, and 3 kernels in each of the three completely linked layers, respectively. By using random gradient descent with momentum, the CNN was trained.Table 3 displays the classification outcomes for the various convolutional layer counts. The best results were produced by the CNN with four convolutional layers, while the performances from three to seven convolutional layers did not significantly differ.

Table 3. Average accuracy by the different number of convolutional layers in Erhai Lake.

The Number of convolutional layers	2	3	4	5	6	7
Average accuracy	89.90%	92.26%	92.49%	92.40%	92.10%	92.09%

We compared CNN's classification performance to that of popular machine-learning models SVM and RF in order to assess its performance. For classification, visual cues such as texture and colour were chosen its shown in fig 9.

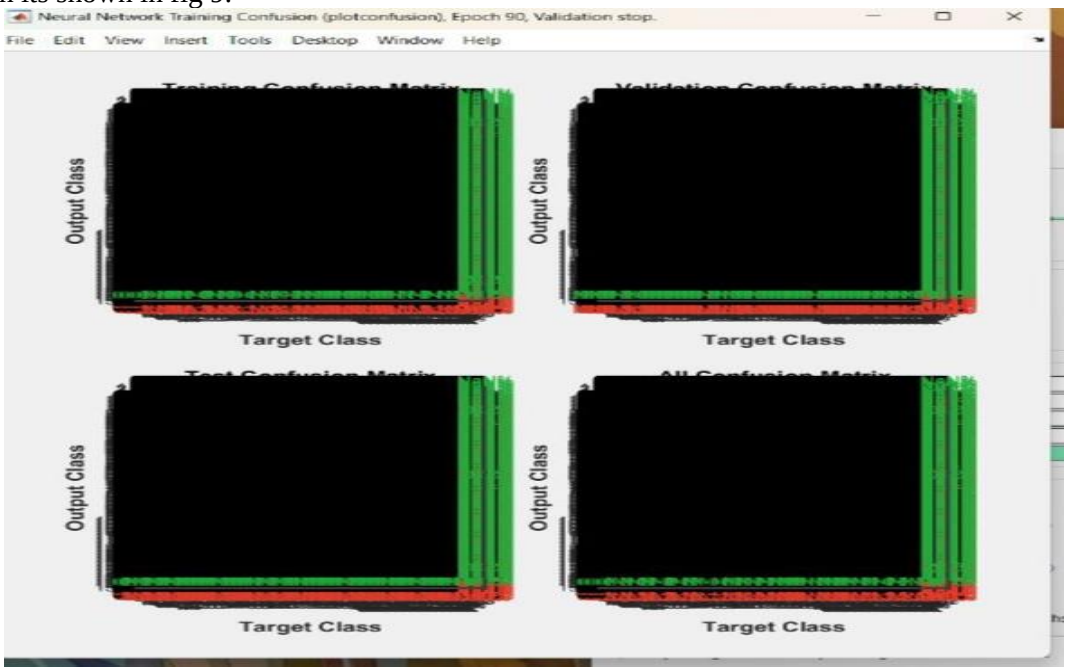

Fig 9: Neural Network Training Conclusion

Fig 10: Error Histogram

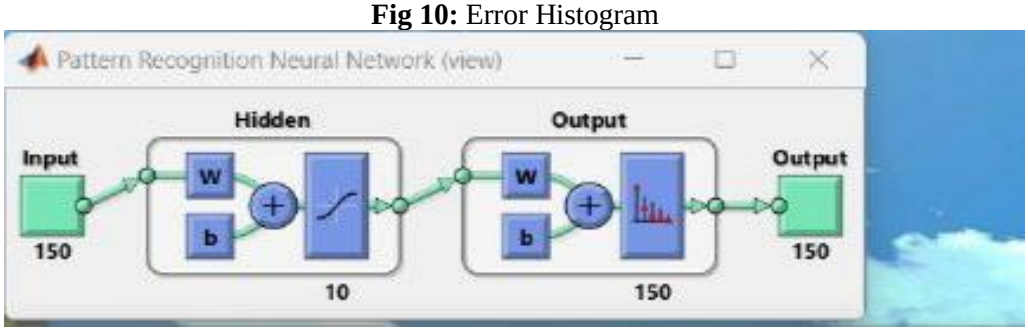

Fig 11: Pattern Recognition

By running your MATLAB code several times in order to warm it up and take into account measurement noise, the MATLAB testing for performance framework enables you to assess the performance of your code. The framework's features allow you to run qualifications within the results of tests to ensure proper functional behaviour in addition to assessing code performance. You can run your performance tests like regular regression tests to make sure that code changes do not invalidate performance tests by utilising the script, function, and class-based unit testing interfaces its shown in fig 10.

A feedforward neural network's post-training error histogram shows the distribution of errors between the target and predicted values. The error values, which can be positive or negative, represent the discrepancy between the goal and projected values its shown in fig 11. The whole range of errors is represented by 30 smaller bits that make up the histogram. On the graph, each bin is represented by a vertical bar, and height of the bar shows how many specimens from the dataset fall into each bin. For instance, a bin with a height of 150 for the training dataset and 150–200 for the verification and test datasets is centred on an error value of 0.001502, respectively. A reference line that represents the error value of zero on the X-axis is known as the zero error line. zero errors point in this instance lies within the bin with a centre value of 0.001502 its shown in fig 12.

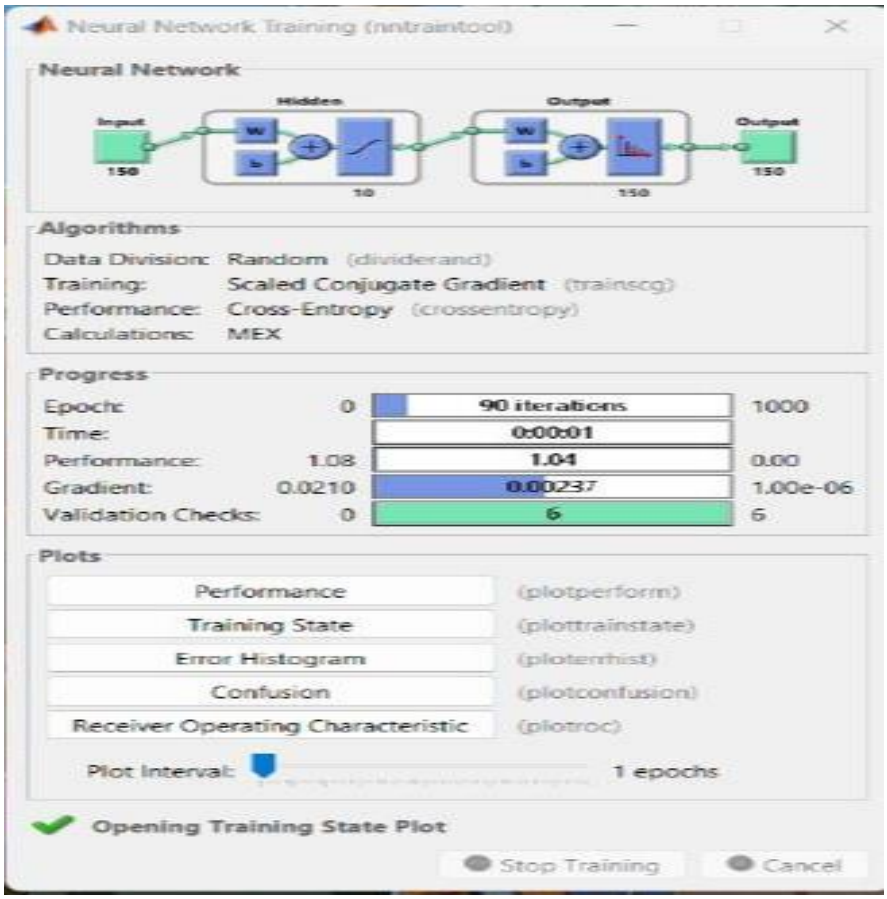

Fig 12: Neural Network Training (n traintool)

The row and column indices of the matrix of confusion C are the same and are placed in the [g1;g2] default sort order as (1,2,3,4). The matrix displays the outcomes of classification for the two groups. All of the data points in group 1 are correctly classified, but one data point from group 2 was incorrectly assigned to group 3 and another from group 3 was incorrectly assigned to group 4 its shown in fig 13a. The confusion matrix C does not contain the NaN value in the grouping variable g2 since it is considered to be missing. Use the confusion chart tool to see the matrix of confusion as a chart its shown in fig 13b.

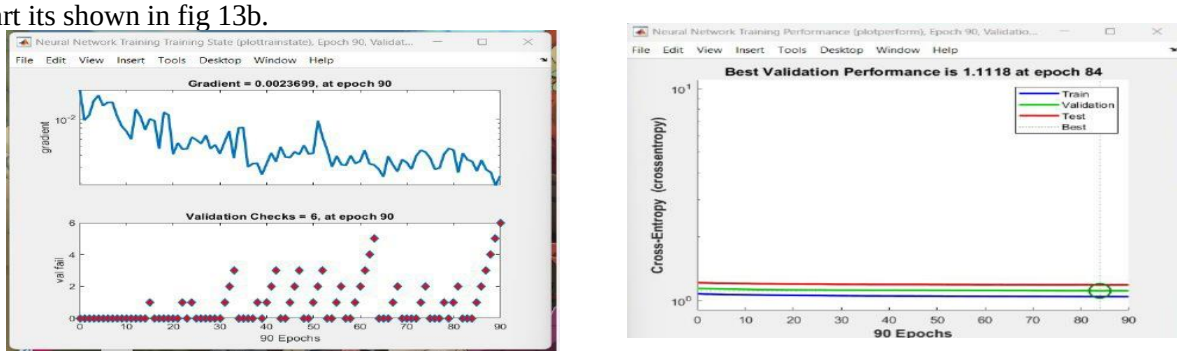

Fig 13 a) Neural Network Training(plottrainstate)**b)**Neural Network Training (plotperform)

The geometry object that results from the translate function's two input inputs, g and s, is returned with a handle, h. The function updates the original geometry if g is a discrete geometric object, and it then returns a handle to the altered discrete geometry object, denoted by h. The old geometry is unaltered if g is an Analytic Geometry object and h is an handle to a new Discrete Geometry object its shown in fig 14.

The receiver operating characteristic (ROC) is a metric used to assess the performance of classifiers. For each class, the roc function applies threshold values over the range [0, 1] to its outputs, and at

each threshold, it calculates two values: the true positive rate (TPR) and the false positive rate (FPR). For a particular class i, TPR is the proportion of outputs whose actual and predicted class is i to the sum of outputs whose actual class i.

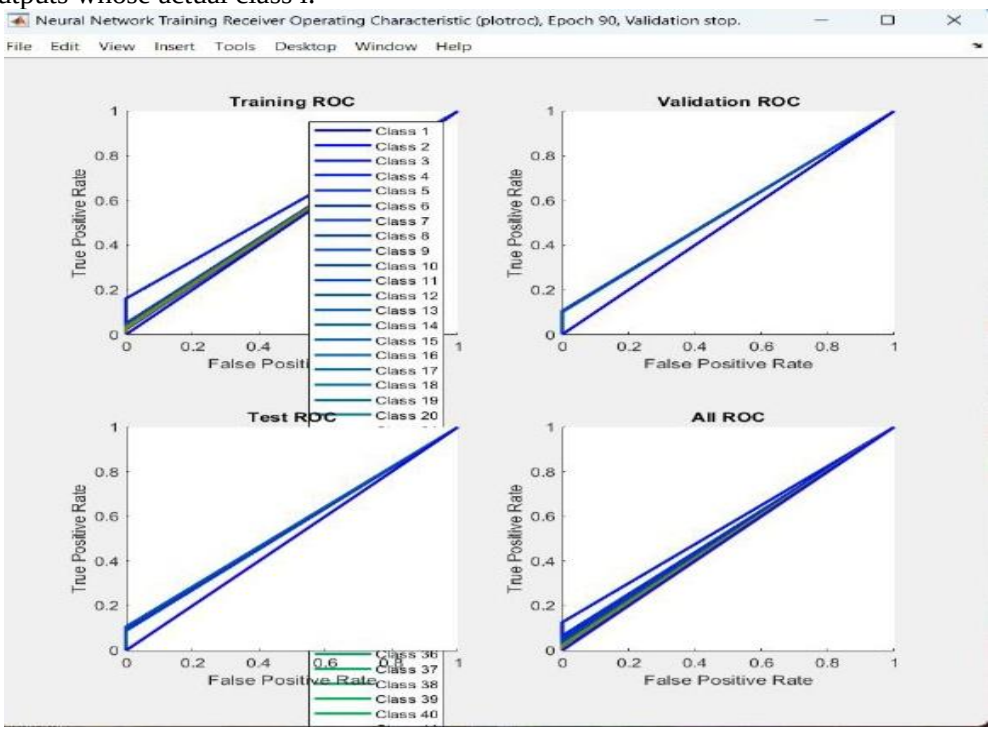

Fig 14: Neural Network Training Receiver Operating Characteristics(plotroc)

The CNN was the most effective way to categorise the water quality of Erhai Lake. Due to its strong learning capabilities, the CNN can extract complex and discriminative features from multispectral images in addition to shallow features like colour and texture. As a result, CNN's classification performance was the best.

5 Conclusion

In this study, we set up an Alex Net-based convolutional neural network to simulate the correlation between in-situ water quality levels and Landsat8 pictures. Four convolutional layers and three fully connected layers made up the CNN. At Erhai Lake, we used in situ monitoring data, spatially and temporally matched Landsat8 images, to train the CNN model. SVM and RF, two conventional machine-learning techniques, CNN had the highest classification accuracyTransfer learning is another benefit of CNN. The approach developed at Erhai Lake could be used to categorise the water quality at Chaohu Lake. Our research suggests that the configured CNN can be used to remotely sense lake water quality and monitor it. Our approach offers an affordable option to increase the spatial-monitoring coverage. It enhances inland-lake monitoring's coverage and accuracy. Our future research will concentrate on enhancing the interpretability of CNN models utilising variables relevant to water quality.

References

1. Su, J.; Ji, D.F.; Mao, L.; Chen, Y.Q.; Sun, Y.Y.; Huo, S.L.; Zhu, J.C.; Xi, B.D. Developing surface water quality standards in China. Resour. Conserv. Recycl. 2016, 117, 294–303.

2. Chen, K.; Ni, M.; Cai, M.; Wang, J.; Huang, D.; Chen, H.; Wang, X.; Liu, M. Optimizatiof a coastalenvironmental monitoring network based on the Kriging method: A case study of quanzhou cay, China.BioMed Res. Int. 2016, 1, 1–12.

3. Hajigholizadeh, M.; Melesse, A.M.; Reddi, L. A comprehensive review on water quality parametersestimation using remote sensing techniques. Sensors 2016, 16, 1298. [PubMed]

4. Nazeer, M.; Bilal, M.; Alsahli, M.M.M.; Shahzad, M.I.; Waqas, A. Evaluation of empirical and machinelearning algorithms for estimation of coastal water quality parameters. Int. J. Geo-Inf. 2017, 6, 360.

5. Du, C.; Wang, Q.; Li, Y.; Lyu, H.; Zhu, L.; Zheng, Z.; Wen, S.; Liu, G.; Guo; Y. Estimation of total phosphorusconcentration using a water classification method in inland water. Int. J. Appl. Earth Obs. Geoinf. 2018, 71,29–42.
6. Yu, X.; Yi, H.; Liu, X.; Wang, Y.; Liu, X.; Zhang, H. Remote-sensing estimation of dissolved inorganic nitrogenconcentration in the Bohai Sea using band combinations derived from MODIS data. Int. J. Remote Sens. 2017,37, 327–340.
7. Singh, A.; Jakubowski, A.; Chidister, I.; Townsend, P.A. A MODIS approach to predicting stream waterquality in Wisconsin. Remote Sens. Environ. 2013, 128, 74–86.
8. Mathew, M.M.; Rao, N.S.; Mandla, V.R. Development of regression equation to study the total nitrogen, totalphosphorus and suspended sediment using remote sensing data in Gujarat and Maharashtra coast of India.J. Coastal Conserv. 2017, 21, 1–11.
9. Politi, E.; Prairie, Y.T. The potential of earth observation in modelling nutrient loading and water quality inlakes of southern Québec, Canada. Aquat. Sci. 2018, 80, 8.
10. Politi, E.; Cutler, M.E.J.; Rowan, J.S. Evaluating the spatial transferability and temporal repeatability ofremote-sensing-based lake water quality retrieval algorithms at the European scale: A meta-analysisapproach. Aquat. Sci. 2015, 36, 3005.
11. Tan, W.X.; Liu, P.C.; Liu, Y.; Yang, S.; Feng, S. A 30-year assessment of phytoplankton blooms in Erhai Lakeusing Landsat imagery: 1987 to 2016. Remote Sens. 2017, 12, 1265.
12. Min, C.; Ning, W.; Li, F. Extraction of water body with different water quality types based on Landsat8image. J. Anhui Agric. Sci. 2016, 30, 220–222.
13. Kuang, R.Y.; Luo, W.; Zhang, M. Optical classification of Poyang Lake waters based on in situ measurementsand remote sensing images. Resour. Environ. Yangtze Basin 2015, 5, 1.
14. Vapnik, V.V. The nature of statistical learning theory. In The Nature of Statistical Learning Theory; Springer:Berlin, Germany, 2000.
15. Zhou, Y.; Chen, Y.H.; Feng, L.; Zhang, X.; Shen, Z.F.; Zhou, X.C. Supervised and adaptive feature weightingfor object-based classification on satellite images. IEEE J. Sel. Top. Appl. Earth Obs. Remote Sens. 2018, 99, 1–11.
16. Cutler, A.; Cutler, D.R.; Stevens, J.R. Random forests. Mach. Learn. 2011, 45, 157–176.
17. Tong, X.Y.; Lu, Q.K.; Xia, G.S.; Zhang, L.P. Large-scale land cover classification in GaoFen-2 satellite imagery.In Proceedings of the IGARSS 2018—IEEE International Geoscience and Remote Sensing Symposium,Valencia, Spain, 22–27 July 2018.
18. Zhang, L.P.; Zhang, L.F.; Du, B. Deep learning for eemote sensing data: A technical tutorial on the State ofthe art. IEEE Geosci. Remote Sens. Mag. 2016, 4, 22–40.
19. Haut, J.M.; Paoletti, M.E.; Plaza, J.; Li, J.; Plaza, A.; Chen, H.; Wang, X.; Liu, M. Active learning withconvolutional neural networks for hyperspectral image classification using a new Bayesian approach.IEEE Trans. Geosci. Remote Sens. 2018, 99, 1–22.
20. Zhao, W.; Jiao, L.C.; Ma, W.P.; Zhao, J.Q.; Zhao, J.; Liu, X.H.; Yang, S.Y. Superpixel-based multiple local CNNfor panchromatic and multispectral image classification. IEEE Trans. Geosci. Remote Sens. 2017, 99, 1–16.
21. Brook, A.; Dor, E.B. Supervised vicarious calibration SVC of hyperspectral remote-sensing data.Remote Sens. Environ. 2011, 115, 1543–1555. Remote Sens. 2019, 11, 1674 14 of 14
22. Lu, D.S.; Mausel, P.; Brondizio, E.S.; Moran, E. Assessment of atmospheric correction methods for LandsatTM data applicable to Amazon basin LBA research. Int. J. Remote Sens. 2002, 23, 2651–2671.
23. Nazeer, M.; Nichol, J. Improved water quality retrieval by identifying optically unique water classes. J. Hydrol2016, 541, 1119–1132.
24. Pyo, J.; Ligaray, M.; Kwon, Y.S.; Ahn, M.H.; Kim, K.; Lee, H.; Kang, T.; Cho, S.B.; Park, Y.; Cho, K.H.High-spatial resolution monitoring of phycocyanin and chlorophyll-a using airborne hyperspectral imagery.Remote Sens. 2018, 10, 1180.
25. Liu, J.M.; Zhang, Y.J.; Yuan, D.; Song, X.Y. Empirical estimation of total nitrogen and total phosphorusconcentration of urban water bodies in china using high resolution IKONOS multispectral imagery. Water2015, 7, 65511–6573.

26. Xu, X.; Huang, X.L.; Zhang, Y.L.; Yu, D. Long-term changes in water clarity in lake Liangzi determined byremote sensing. Remote Sens. 2018, 10, 1441.
27. Liu, D.Z.; Fu, D.Y. Atmospheric correction of Hyperion imagery over estuarine waters: A case study of thePearl River Estuary in southern China. Int. J. Remote Sens. 2017, 38, 199–210.
28. Souleyman, C.; Liu, H.; Gu, Y.F.; Yao, H.X. Deep feature fusion for VHR remote sensing scene classification.IEEE Trans. Geosci. Remote Sens. 2017, 99, 1–10.
29. Cheng, G.; Yang, C.Y.; Yao, X.W.; Li, K.M.; Han, J.W. When deep learning meets metric learning: Remotesensing image scene classification via learning discriminative CNNs. IEEE Trans. Geosci. Remote Sens. 2018,99, 1–11.
30. Krizhevsky, A.; Sutskever, I.; Hinton, G. ImageNet Classification with Deep Convolutional Neural Networks; NIPSCurran Associates, Inc.: Harrahs and Harveys, Lake Taho, NV, USA, 2012.31. Simonyan, K.; Zisserman, M. Very deep convolutional networks for large-scale image recognition. arXiv2014, arXiv:1409.1556.
32. He, K.M.; Zhang, X.Y.; Ren, S.Q.; Sun, J. Deep residual learning for image recognition. In Proceedingsof the 2016 IEEE Conference on Computer Vision and Pattern Recognition (CVPR), Las Vegas, NV, USA,27–30 June 2016.
33. Zeiler, M.D.; Fergus, R. Visualizing and understanding convolutional networks. In European Conference onComputer Vision; Springer: Cham, Switzerland, 2013.
34. Srivastava, N.; Hinton, G.; Krizhevsky, A.; Sutskever, I.; Salakhutdinov, R. Dropout: A simple way to preventneural networks from overfitting. J. Mach. Learn. Res. 2014, 15, 1929–1958.
35. Yosinski, J.; Clune, J.; Bengio, Y.; Lipson, H. How transferable are features in deep neural networks? arXiv2014, arXiv:1411.1792.
36. Saeed, A.; Khan, A.; Zameer, A.; Usman, A. Wind power prediction using deep neural network based metaregression and transfer learning. Appl. Soft Comput. 2017, 58, 742–755.
37. Ojala, T.; Pietikainen, M.; Harwood, D. A comparative study of texture measures with classification based onfeature distributions. Pattern Recognit. 1996, 29, 51–59.
38. Haralick, R.M.; Shanmugam, K.; Dinstein, I. Textural features for image classification. Stud. Media Commun.1990, 3, 610–621.
39. Yu, G.L.; Yang, W.; Matsushita, B.; Li, R.H.; Oyama, Y.; Fukushima, T. Remote estimation of chlorophyll-a ininland waters by a NIR-red-based algorithm: Validation in Asian Lakes. Remote Sens. 2014, 4, 3492–3510.
40. Wu, L.; Wang, L.; Min, L.; Hou, W.; Guo, Z.W.; Zhao, J.H.; Li, N. Discrimination of algal-bloom usingspaceborne SAR observations of Great Lakes in China. Remote Sens. 2018,5, 767.